

Runge–Kutta–Nyström symplectic splitting methods of order 8

S. Blanes¹, F. Casas², A. Escorihuela-Tomàs³

¹ *Universitat Politècnica de València, Instituto de Matemática Multidisciplinar, 46022-Valencia, Spain
email: serblaza@imm.upv.es*

² *Departament de Matemàtiques and IMAC, Universitat Jaume I, 12071-Castellón, Spain
email: Fernando.Casas@mat.uji.es*

³ *Departament de Matemàtiques, Universitat Jaume I, 12071-Castellón, Spain
email: alescori@uji.es*

February 4, 2022

Abstract

Different families of Runge–Kutta–Nyström (RKN) symplectic splitting methods of order 8 are presented for second-order systems of ordinary differential equations and are tested on numerical examples. They show a better efficiency than state-of-the-art symmetric compositions of 2nd-order symmetric schemes and RKN splitting methods of orders 4 and 6 for medium to high accuracy. For some particular examples, they are even more efficient than extrapolation methods for high accuracies and integrations over relatively short time intervals.

Keywords: Runge–Kutta–Nyström splitting methods, high order symplectic integrators

1 Introduction

Second-order systems of ordinary differential equations (ODEs) of the form

$$\ddot{y} \equiv \frac{d^2y}{dt^2} = g(y), \quad (1.1)$$

where $y \in \mathbb{R}^d$ and $g : \mathbb{R}^d \rightarrow \mathbb{R}^d$, appear very often in applications, so that special numerical integrators have been designed for them, such as the Runge–Kutta–Nyström (RKN) class of methods. As is well known, if one introduces the new variables $x = (y, v = \dot{y})$ and the maps

$$f_a(x) = f_a(y, v) = (v, 0), \quad f_b(x) = f_b(y, v) = (0, g(y)), \quad (1.2)$$

then eq. (1.1) is equivalent to

$$\dot{x} = f_a(x) + f_b(x) \quad (1.3)$$

and moreover each subsystem $\dot{x} = f_i(x)$, $i = a, b$, is explicitly integrable, with exact flow

$$\varphi_t^{[a]}(y, v) = (y + tv, v) \quad \text{and} \quad \varphi_t^{[b]}(y, v) = (y, v + tg(y)),$$

respectively. An important class of problems leading to equations of the form (1.1) corresponds to Hamiltonian dynamical systems of the form

$$H(q, p) = \frac{1}{2}p^T M^{-1}p + V(q), \quad (1.4)$$

where q and p denote coordinates and momenta, respectively, M is a symmetric positive definite square constant matrix and $V(q)$ is the potential. Then, the corresponding equations of motion can be written as (1.1) with $y = q$, $v = \dot{y} = Mp$ and $g(y) = -M\nabla V(q)$.

Splitting methods constitute a natural option for integrating numerically the initial value problem defined by (1.3). These are schemes of the form

$$\psi_h = \varphi_{ha_s}^{[a]} \circ \varphi_{hb_s}^{[b]} \circ \dots \circ \varphi_{ha_1}^{[a]} \circ \varphi_{hb_1}^{[b]}, \quad (1.5)$$

where the coefficients a_j, b_j are conveniently chosen so as to achieve high order approximations to the exact flow of (1.3), namely $\varphi_h(x) = \psi_h(x) + \mathcal{O}(h^{r+1})$ for a given order r and step size h . Familiar examples of splitting methods are the so-called Strang/leapfrog/Störmer–Verlet second order schemes:

$$\mathcal{S}_h^{[2]} = \varphi_{h/2}^{[a]} \circ \varphi_h^{[b]} \circ \varphi_{h/2}^{[a]}, \quad (1.6)$$

and

$$\mathcal{S}_h^{[2]} = \varphi_{h/2}^{[b]} \circ \varphi_h^{[a]} \circ \varphi_{h/2}^{[b]}. \quad (1.7)$$

In fact, efficient schemes of this class up to order $r = 6$ have been designed along the years (see e.g. [5] and references therein). In addition, they preserve qualitative properties of the continuous system and show a very good behavior with respect to the propagation of errors, especially for long time integrations [11].

There are situations, however, when even higher-order numerical approximations ($r = 8, 10, \dots$) are required, for instance in problems arising in astrodynamics. In that case, although generic splitting methods exist, they involve such a large number of elementary flows $\varphi_h^{[a]}, \varphi_h^{[b]}$, that are not competitive with other integrators. This is so due to the exponential growth with the order r of the required number of conditions to be satisfied to achieve that order [19]. For this reason, palindromic compositions of the form

$$\mathcal{S}_{\alpha_m h}^{[2]} \circ \mathcal{S}_{\alpha_{m-1} h}^{[2]} \circ \dots \circ \mathcal{S}_{\alpha_2 h}^{[2]} \circ \mathcal{S}_{\alpha_1 h}^{[2]} \quad \text{with} \quad (\alpha_1, \dots, \alpha_m) \in \mathbb{R}^m \quad (1.8)$$

and $\alpha_{m+1-i} = \alpha_i$, have been considered instead for order $r > 6$. In practice, schemes (1.8) are the most realistic option when one is interested in integrating (1.3) with high-order ($r = 8, 10, \dots$) splitting methods.

It turns out, however, that the special structure of (1.2)-(1.3) corresponding to the system (1.1) leads to a reduction in the number of order conditions when $r > 4$ with respect to the generic problem. This allows one to construct highly efficient 4th- and 6th-order splitting methods especially tailored for this class of problems which show a better performance than schemes of the family (1.8) [8, 24]. They can be naturally called *RKN splitting methods*, and the question of the existence of eighth-order schemes, more efficient than methods of type (1.8), formulated some 25 years ago [21, p. 153], still remains unanswered, no doubt due to the technical difficulties involved.

It is our purpose in this note to present new RKN splitting methods of order 8 that provide higher efficiency than state-of-the-art composition methods (1.8) on a variety of examples arising in physical applications. They should then be considered as the natural option when one is interested in integrating numerically problems of the form (1.2)-(1.3) with medium to high precision whereas preserving by construction the main qualitative features of the continuous system.

Remark 1.1 *It turns out that this class of schemes can also be used to solve the slightly more general problem*

$$\ddot{y} = \alpha \dot{y} + \beta y + g(t, y), \quad (1.9)$$

where $\alpha, \beta \in \mathbb{R}^{d \times d}$ are constant: by taking time t as a new coordinate and considering $x = (y, v, t)$, it is clear that equation (1.9) can be again expressed as (1.3), this time with

$$f_a(x) = f_a(y, v, t) = (v, \alpha v + \beta y, 1), \quad f_b(x) = f_b(y, v, t) = (0, g(t, y), 0), \quad (1.10)$$

and each sub-system being explicitly integrable.

2 Order conditions

As shown e.g. in [4], to each integrator (1.5) one can associate a series $\Psi(h)$ of differential operators given by

$$\Psi(h) = \exp(hb_1 F_b) \exp(ha_1 F_a) \cdots \exp(hb_s F_b) \exp(ha_s F_a), \quad (2.1)$$

where F_a, F_b are the Lie derivatives corresponding to f_a and f_b , respectively [3]: for each smooth function $g : \mathbb{R}^d \rightarrow \mathbb{R}^d$ and $x \in \mathbb{R}^d$ one has

$$F_a g(x) = f_a(x) \cdot \nabla g(x), \quad F_b g(x) = f_b(x) \cdot \nabla g(x), \quad (2.2)$$

so that, for the whole integrator, $g(\psi_h(x)) = \Psi(h)g(x)$. For $g(x) = (g_1(x), \dots, g_d(x))$, we denote

$$f(x) \cdot \nabla g(x) \equiv (f(x) \cdot \nabla g_1(x), \dots, f(x) \cdot \nabla g_d(x))$$

in eq. (2.2). The main advantage of using the series $\Psi(h)$ for representing the method ψ_h is that one can formally apply the Baker–Campbell–Hausdorff formula [28] and express $\Psi(h)$ as only one exponential,

$$\Psi(h) = \exp(F(h)), \quad \text{with} \quad F(h) = \sum_{j \geq 1} h^j F_j, \quad (2.3)$$

and each F_j is a linear combination of nested commutators involving j operators F_a and F_b whose coefficients are polynomials of degree j in the coefficients a_i, b_i . A method of order r requires that $F_1 = F_a + F_b$ for consistency, and $F_j = 0$ for $1 < j \leq r$. These constraints in turn lead to a set of polynomial equations to be satisfied by the coefficients of the splitting method. The number n_r of such order conditions at each r is collected in Table 1 [19]. For comparison, we also include the number s_r of order conditions for compositions of the form (1.8)

As is well known, if the composition (1.5) is left-right palindromic, then all the order conditions at even order are automatically satisfied and the method is time-symmetric. For systems of the form (1.2)-(1.3), the flow $\varphi_h^{[b]}$ is typically the most expensive part to evaluate (for the Hamiltonian (1.4), it corresponds essentially

r	1	2	3	4	5	6	7	8	9	10
s_r	1	0	1	1	2	2	4	5	8	11
n_r	2	1	2	3	6	9	18	30	56	99
ℓ_r	2	1	2	2	4	5	10	14	25	39

Table 1: Number of independent order conditions (at order r) of compositions of symmetric second order methods of the form (1.8), s_r , of splitting methods in the general case, n_r , and in the RKN case, ℓ_r .

to the force $\nabla V(q)$). It makes sense, then, to characterize a given splitting method according to the number of flows $\varphi_h^{[b]}$ involved. This is called the *number of stages* of the method. Notice that, if the Strang splitting is used as the scheme $\mathcal{S}_h^{[2]}$ in the composition (1.8), the number of stages is also m .

From Table 1 it is then straightforward to estimate the minimum number of stages to achieve an even order $r = 2k$. For the composition (1.8) and the general splitting (1.5) these values are, respectively,

$$S_r = 2 \sum_{i=1}^k s_{2k-1} - 1, \quad N_r = \sum_{i=1}^k n_{2k-1} - 1,$$

and are collected in Table 2 up to $r = 2k = 10$. Notice that, when counting the number of stages per step, we have used the so-called FSAL (First Same As Last) property: the last map in one step can be saved in the following one and does not count for the total number of stages.

r	2	4	6	8	10
S_r	1	3	7	15	31
N_r	1	3	9	27	83
L_r	1	3	7	17	42

Table 2: Minimum number of stages required to achieve order $r = 2k$ with symmetric compositions (1.8), S_r , with general splitting (1.5), N_r , and for RKN splitting methods, L_r .

The number of order conditions to be solved for each family of methods is, respectively, $(S_r + 1)/2$ and $N_r + 1$. It is clear that symmetric compositions (1.8) require to solve a considerably smaller number of order conditions to achieve high order methods. On the other hand, the space of solutions is significantly larger in the case of general splitting methods, and consequently also the chance of finding highly efficient schemes within this class. Thus, in particular, the general splitting methods of order four and six presented in [8] outperform compositions (1.8) of the same order. At order eight, however, one has to solve a system of 28 polynomial equations for general splitting methods, and although it seems quite likely that very efficient solutions exist, to carry out a thorough analysis constitutes a formidable task.

Notice that for systems of the form (1.2)-(1.3) one has further restrictions: since $F_a = v \nabla_y$, and $F_b = g(y) \nabla_v$, one has for symmetric methods

$$[F_b, [F_a, F_b]] = \tilde{g}(y) \nabla_v, \quad \text{with} \quad \tilde{g}(y) = 2 \nabla_y g(y) \cdot g(y),$$

where $[F_a, F_b] = F_a F_b - F_b F_a$, etc. In consequence, $[F_b, [F_b, [F_a, F_b]]] \equiv 0$, and many terms in (2.3) vanish identically, so that their order conditions can be ignored. This can be seen in the last row of Tables 1 and 2,

where we collect the order conditions ℓ_r and the the minimum number of stages,

$$L_r = \sum_{i=1}^k \ell_{2k-1} - 1$$

up to $r = 10$. Notice that, whereas the reduction up to $r = 6$ with respect to general splitting methods is only of two equations, for a time-symmetric method of order $r = 8$ one has to solve 18 order conditions (instead of 28). This problem, although more amenable, is still far from trivial. In addition, to get significant solutions, the relevant issue here is whether the resulting 8th-order RKN splitting schemes are competitive in terms of the number of flows involved with methods within the class (1.8).

Remark 2.1 *With respect to the more general system (1.9)-(1.10), one has*

$$F_a = v \nabla_y + (\alpha v + \beta y) \nabla_v + 1 \cdot \partial_t, \quad F_b = g(t, y) \nabla_v,$$

so that

$$[F_b, [F_a, F_b]] = \tilde{g}(t, y) \nabla_v, \quad \text{with} \quad \tilde{g}(y) = 2 \nabla_y g(t, y) \cdot g(t, y)$$

and therefore $[F_b, [F_b, [F_a, F_b]]] \equiv 0$ also here.

Before starting a systematic search of solutions to the order conditions, it seems appropriate to make explicit several considerations:

1. Due to the different qualitative character of the operators F_a and F_b , it is clear that the role of $\varphi_h^{[a]}$ and $\varphi_h^{[b]}$ in (1.5) is not interchangeable, and so two different orderings have to be considered. Specifically, we will analyze two types of composition:

$$\mathcal{A}_s = \varphi_{ha_{s+1}}^{[a]} \circ \varphi_{hb_s}^{[b]} \circ \varphi_{ha_s}^{[a]} \circ \cdots \circ \varphi_{hb_1}^{[b]} \circ \varphi_{ha_1}^{[a]}, \quad (2.4)$$

with $a_{s+2-i} = a_i$, $b_{s+1-i} = b_i$, and

$$\mathcal{B}_s = \varphi_{hb_{s+1}}^{[b]} \circ \varphi_{ha_s}^{[a]} \circ \varphi_{hb_s}^{[b]} \circ \cdots \circ \varphi_{ha_1}^{[a]} \circ \varphi_{hb_1}^{[b]}, \quad (2.5)$$

with $b_{s+2-i} = b_i$, $a_{s+1-i} = a_i$. Since for methods (2.4) and (2.5) one can always apply the FSAL property, we say that both schemes involve the same number s of stages.

2. Very often, compositions with a higher number of stages than the minimum required to solve the order conditions are considered in the literature. This is so because, typically, (i) methods with the minimum number of stages show a poor performance, and (ii) the presence of free parameters allows one to optimize the schemes according with some appropriate criteria, so that the extra computational cost is compensated by the reduction in the error. Thus, in particular, 8th-order methods within the class (1.8) with 17, 19 and 21 stages exist that are more efficient than schemes with the minimum number $m = 15$. Notice in this respect that the minimum number of stages for a RKN splitting method of order 8 is $s = 17$. Although one such method of the form \mathcal{A}_s was proposed in [23], the numerical results collected there show no clear improvement with respect to the 8th-order method of type (1.8) with $m = 24$ presented in [9].

3. Given a method ψ_h , one may consider a near-to-identity map π_h so that the integrator $\hat{\psi}_h = \pi_h^{-1} \circ \psi_h \circ \pi_h$ is more accurate than ψ_h , for instance, by increasing its order. In this context, ψ_h is called the kernel of the processed method $\hat{\psi}_h$, and π_h is the processor or corrector. Notice that N consecutive steps correspond to $\hat{\psi}_h^N = \pi_h^{-1} \circ \psi_h^N \circ \pi_h$, i.e., the cost of applying the processed scheme is basically the cost of the kernel. This technique allows one to separate the order conditions into two sets: the conditions satisfied by the kernel itself, and those to be verified by the processor. As a result, it is possible to construct high-order RKN splitting methods involving a reduced number of stages in the kernel, although building a particular processor is far from trivial. Methods of this class have been presented in [6, 7], so that they will not be considered here.
4. For the initial value problem defined by (1.2)-(1.3), it is possible to include in the compositions (2.4) and (2.5) the flows generated by other vector fields lying in the Lie algebra generated by F_a and F_b . For instance, one could use the h -flow of the vector fields $[F_b, [F_a, F_b]]$, $[F_b, [F_b, [F_a, [F_a, F_b]]]]$, and other more general nested commutators [6, 7]. These give rise to the so-called ‘modified potentials’, and allow one to reduce the number of stages (although at the price of an additional computational cost to evaluate the flows). Methods of this class with and without processing have been analyzed in particular in [6] and [24]. Here, by contrast, we are only interested in standard compositions (2.4)-(2.5).

3 New methods of order 8

We next analyze families of schemes (2.4) and (2.5) involving $s = 17, 18$ and 19 stages, so that one always has enough parameters in the compositions to solve the order conditions. Of course, even with the minimum number of parameters, these order conditions possess a large number of real solutions, so that some criterion has to be adopted to select “good” methods. As is customary in the literature, and assuming h is sufficiently small and g is sufficiently smooth, we propose to take the leading term in the asymptotic expansion of the modified vector field associated with the integrator as the main contribution to the truncation error. Without any specific assumption on the function g , we take this error as $(\sum_{i=1}^{25} k_{9,i}^2)^{1/2}$. Here $k_{9,i}$ are the coefficients of the asymptotic expansion of the modified vector field at order h^9 when it is expressed as a linear combination of the 25 independent nested commutators involving 9 operators F_a and F_b . This corresponds to the subspace of the Lie algebra generated by F_a and F_b with the commutator as the Lie bracket (for more details, see [20, 18]). To take into account the computational cost, we multiply this error by the number of stages s , thus resulting in the following effective error for a method of order 8,

$$E_f = s \cdot \left(\sqrt{\sum_{i=1}^{25} k_{9,i}^2} \right)^{1/8}, \quad (3.1)$$

which should be minimized by the integrator. One has to take into account, however, that the expression of E_f depends on the particular basis of nested commutators one is considering and that we are also assuming that all these commutators contribute in a similar way, something that is not guaranteed to take place in all applications. It makes sense, then, to introduce other quantities as possible estimators of the error committed. In particular, it has been noticed that large coefficients a_i, b_i in the splitting method usually leads to large truncation errors, since the expressions of $k_{\ell,j}$ for $\ell \geq 9$ depend on increasingly higher powers of these

coefficients. For this reason, we also keep track of the quantities

$$\Delta \equiv \sum_{i=1}^s (|a_i| + |b_i|) \quad \text{and} \quad \delta \equiv \max_{i=1}^s (|a_i|, |b_i|) \quad (3.2)$$

and eventually discard solutions with large values of Δ and/or δ . By following a similar approach as for instance in [8, 24], we will select particular schemes with small values of E_f , Δ and δ , and then we will test them on an array of numerical examples to check their efficiency in practice.

$s = 17$ stages. In this case one has as many parameters as order conditions, 18 in total. Given the complexity of the problem, it is not possible to solve these nonlinear equations with a computer algebra system, and so one has to turn to numerical techniques. Specifically, they are solved with the Python [27] function `fsolve` of the *SciPy* library [29], a wrapper of the classic subroutines HYBRD and HYBRJ of MINPACK [22]. The algorithm is based on a modification of the Powell hybrid method and involves the choice of the correction as a convex combination of the Newton method and scaled gradient directions and the updating of the Jacobian by the rank-1 method (except at the starting point, where it is approximated by forward differences). Since we are not interested in methods with large values of δ , a uniform distribution in the interval $[-1, 1]$ in each variable was taken to generate about 2×10^6 initial points to start the procedure,

When a composition of type \mathcal{A}_s is considered, we have obtained 376 real solutions that cannot be obtained as a composition of 2nd-order symmetric schemes (1.8), with parameters $E_f \in [2.77, 18.05]$ and $\Delta \in [8.40, 63.05]$, respectively. Among these, we select those solutions within the more restricted range $E_f \in [2.86, 3.45]$ and $\Delta \in [8.42, 19.30]$ and check them on the test problems of sections 4 and 5. Finally, we have chosen the scheme whose coefficients are listed in Table 4, and parameters given in Table 3. The final values of the coefficients (with 30 digits of accuracy) have been obtained by taking the solution found by `fsolve` as the starting point of the function `FindRoot` of *Mathematica*. The method can be represented in the compact form

$$\mathcal{A}_{17} \equiv (a_1, b_1, a_2, b_2, a_3, b_3, a_4, b_4, a_5, b_5, a_6, b_6, a_7, b_7, a_8, b_8, a_9, b_9, a_9, b_8, a_8, b_7, a_7, b_6, a_6, b_5, a_5, b_4, a_4, b_3, a_3, b_2, a_2, b_1, a_1). \quad (3.3)$$

For compositions of type \mathcal{B}_s , by applying the same methodology, we have found 149 different solutions out of more than 1.2×10^6 starting points. We have selected the four solutions in the region $E_f \in [2.80, 3.85]$, $\Delta \in [7.30, 9.95]$ and finally we take the one whose coefficients are collected in Table 5. The method thus reads

$$\mathcal{B}_{17} \equiv (b_1, a_1, b_2, a_2, b_3, a_3, b_4, a_4, b_5, a_5, b_6, a_6, b_7, a_7, b_8, a_8, b_9, a_9, b_9, a_8, b_8, a_7, b_7, a_6, b_6, a_5, b_5, a_4, b_4, a_3, b_3, a_2, b_2, a_1, b_1). \quad (3.4)$$

$s = 18$ stages. With one more stage we have one free parameter that can be used to get in principle smaller values of the effective error and eventually more efficient schemes, as is common in the literature. Notice that the problem in this case involves solving a system of 18 polynomial equations with 19 variables. Our strategy is the following: for a composition of type \mathcal{A}_s with $s = 18$, we take a_1 as the free parameter, and explore the interval $a_1 \in [0, 1]$ (since we are interested in small values of the coefficients) by fixing each time

	E_f	Δ	δ
\mathcal{A}_{17}	3.45	8.42	0.5459 ($ a_9 $)
\mathcal{A}_{18}	3.65	7.42	0.6406 ($ a_9 $)
\mathcal{A}_{19}	2.76	5.98	0.4237 ($ a_4 $)
\mathcal{B}_{17}	2.80	8.93	0.6355 ($ a_5 $)
\mathcal{B}_{18}	3.44	9.68	0.9303 ($ a_4 $)
\mathcal{B}_{19}	3.41	6.94	0.5238 ($ a_6 $)

Table 3: Effective error E_f , 1- and ∞ -norm of the vector of coefficients for different 8th-order RKN splitting methods of type \mathcal{A}_s and \mathcal{B}_s .

the value of a_1 . Starting with 2×10^6 initial points, we have found 722 valid solutions, the most promising corresponding to the choice $a_1 = 0.08$. This solution is then taken as the starting point of an arc-length continuation method and follow the solution along the curve leading to a local minimum of the 1-norm of the vector of coefficients. In doing so we apply the algorithm presented in [1, 2]. After this process, we check several methods in practice and finally the solution \mathcal{A}_{18} collected in Table 4, with E_f , Δ and δ given in Table 3.

The same technique is applied to compositions \mathcal{B}_{18} leading to the solution collected in Table 5 after 1070748 initial points and the application of arc-length continuation.

$s = 19$ stages. Adding an additional stage and so forming the composition \mathcal{A}_{19} , we have explored the space of parameters in the region $a_1, a_2 \in [0.05, 0.15]$, where we have found 295 valid solutions. Then, we start from the one with best parameters and apply the following strategy: let us denote by \mathbf{u}_0 the vector of coefficients of this initial solution. Then we generate a random vector α verifying $\alpha \cdot (\mathbf{u} - \mathbf{u}_0) = 0$. Now we apply continuation along the curve that results from the intersection of the space of solutions (with 2 free parameters) with the random generated hyperplane. The final solution is collected in Table 5.

Concerning the composition \mathcal{B}_{19} , 173 solutions have been obtained out of more than 1.3×10^6 initial points. After applying the previous technique, we arrive at the solution reported in Table 5.

Although the quantities (3.1) and (3.2) provide useful information about the quality and relative performance of the methods, one should have in mind that the size of the error terms and therefore the efficiency of each scheme ultimately depends on the particular problem one is considering and even on the initial conditions. For this reason it is convenient to check the behavior of the different schemes on a variety of differential equations and initial conditions, and also to compare them with other efficient numerical integrators available in the literature. We have separated the numerical illustrations into two sections. Thus, in section 4 we compare the new schemes with symmetric compositions (1.8) of order 8, whereas in section 5 we also consider RKN splitting integrators of orders 4 and 6, as well as extrapolation methods.

	a_i	b_i
\mathcal{A}_{17}	$a_1 = 0.0520924343840339006426037968353$	$b_1 = 0.145850304812644731608096609877$
	$a_2 = 0.225287493267702165807274831864$	$b_2 = 0.255156544139293944162028807345$
	$a_3 = 0.416276189612257117795363856737$	$b_3 = 0.0181334688208317251361460684041$
	$a_4 = -0.384567270213950399652168569029$	$b_4 = -0.179040110299264554587007062749$
	$a_5 = 0.0997271783470514816674547589369$	$b_5 = -0.118470801433302245053382954342$
	$a_6 = -0.108833834399100218757003157958$	$b_6 = 0.186461689273821083344937258279$
	$a_7 = 0.222010736648991680848341975522$	$b_7 = 0.459041581767136840219244627361$
	$a_8 = 0.523879522036734296002247438223$	$b_8 = -0.003660836270318358975321459399$
	$a_9 = \frac{1}{2} - \sum_{i=1}^8 a_i$	$b_9 = 1 - 2 \sum_{i=1}^8 b_i$
\mathcal{A}_{18}	$a_1 = 0.0866003822712445920135805954462$	$b_1 = -0.08$
	$a_2 = -0.0231572735424388070228714693753$	$b_2 = 0.209460550048243262121199483001$
	$a_3 = 0.191410576083774088999564416369$	$b_3 = 0.274887805875735483503233064415$
	$a_4 = 0.378895558692931579545387584925$	$b_4 = -0.224214208870409561366168655624$
	$a_5 = -0.0467359566364556111599485526051$	$b_5 = 0.347657740563761656321390026010$
	$a_6 = -0.156198111997810415438979605642$	$b_6 = -0.168783183866211679175007668385$
	$a_7 = 0.156025836895094823718831871041$	$b_7 = 0.144209344805460873709120777707$
	$a_8 = 0.252844012473796333586850465807$	$b_8 = 0.0116851121360265483381405054244$
	$a_9 = -0.640644212172254239866860564270$	$b_9 = \frac{1}{2} - \sum_{i=1}^8 b_i$
	$a_{10} = 1 - 2 \sum_{i=1}^9 a_i$	
\mathcal{A}_{19}	$a_1 = 0.0505805$	$b_1 = 0.129478606560536730662493794395$
	$a_2 = 0.149999$	$b_2 = 0.222257260092671143423043559581$
	$a_3 = -0.0551795510771615573511026950361$	$b_3 = -0.0577514893325147204757023246320$
	$a_4 = 0.423755898835337951482264998051$	$b_4 = -0.0578312262103924910221345032763$
	$a_5 = -0.213495353584659048059672194633$	$b_5 = 0.103087297437175356747933252265$
	$a_6 = -0.0680769774574032619111630736274$	$b_6 = -0.140819612554090768205554103887$
	$a_7 = 0.227917056974013435948887201671$	$b_7 = 0.0234462603492826276699713718626$
	$a_8 = -0.235373619381058906524740047732$	$b_8 = 0.134854517356684096617882205068$
	$a_9 = 0.387413869179878047816794031058$	$b_9 = 0.0287973821073779306345172160211$
	$a_{10} = \frac{1}{2} - \sum_{i=1}^9 a_i$	$b_{10} = 1 - 2 \sum_{i=1}^9 b_i$

Table 4: Coefficients of 8th-order RKN splitting methods of type \mathcal{A}_s , with $s = 17, 18$ and 19 stages.

4 Numerical tests I: 8th-order schemes

The first set of examples is intended to illustrate the performance of the new RKN splitting methods in comparison with the most efficient symmetric compositions of the form (1.8) we have found in the literature. In addition, we also include in the tests the only 8th-order RKN splitting method with 17 stages. Specifically, in addition to the previous \mathcal{A}_s and \mathcal{B}_s schemes, we consider the following 8th-order integrators:

	a_i	b_i
\mathcal{B}_{17}	$a_1 = 0.160227696073839513690970240076$	$b_1 = 0.0514196142537210073343152693459$
	$a_2 = 0.306354507436867319879440957100$	$b_2 = 0.250497030318342871458417941091$
	$a_3 = 0.308395508895171191756544975556$	$b_3 = 0.512412268300327350035492806653$
	$a_4 = 0.120362086566233408450063177659$	$b_4 = -0.231597138650894401279645184364$
	$a_5 = -0.622888687549183872072186218718$	$b_5 = 0.116091323536875759881216298975$
	$a_6 = 0.635560951632990078378672016548$	$b_6 = -0.0098365173246965763985763034283$
	$a_7 = -0.144226974795419229640437363913$	$b_7 = -0.108032771466281638634277563747$
	$a_8 = -0.284867527074173816678992817545$	$b_8 = 0.249039864198023642002940910070$
	$a_9 = 1 - 2 \sum_{i=1}^8 a_i$	$b_9 = \frac{1}{2} - \sum_{i=1}^8 b_i$
\mathcal{B}_{18}	$a_1 = 0.144410089394373457971755553148$	$b_1 = 0.045$
	$a_2 = 0.911935520865154315536815857376$	$b_2 = 0.459016679491512416807266107555$
	$a_3 = -0.00072932909837392655161199996844$	$b_3 = -0.0456553445594333153223655352757$
	$a_4 = -0.930317101800698721159455541447$	$b_4 = 0.0457031020401841003192648096559$
	$a_5 = 0.253804074671714046593439154323$	$b_5 = -0.216814341025322492810152535338$
	$a_6 = 0.147948981530918626913598733391$	$b_6 = 0.163168264552484857133047358600$
	$a_7 = -0.448814759614614928125216243784$	$b_7 = -0.0857080319814376219389850039430$
	$a_8 = 0.0824123980794580106751237195418$	$b_8 = 0.0265745810650523466142922093591$
	$a_9 = \frac{1}{2} - \sum_{i=1}^8 a_i$	$b_9 = -0.0365538332992893220147096150675$
	$a_{10} = 1 - 2 \sum_{i=1}^9 a_i$	$b_{10} = 1 - 2 \sum_{i=1}^9 b_i$
\mathcal{B}_{19}	$a_1 = 0.337548675291317241942440116575$	$b_1 = 0.036132460472136313416730168194$
	$a_2 = -0.223647977575409990331768222380$	$b_2 = 0.012697863961074113381675193011$
	$a_3 = 0.168949714872223740906385138015$	$b_3 = 0.201318391240629276109068041836$
	$a_4 = 0.171179938816205886154783136334$	$b_4 = 0.135683350134504233201330671671$
	$a_5 = -0.349765168067292877221144631312$	$b_5 = -0.0579071833999963041504740663015$
	$a_6 = 0.523808861006312397712070357524$	$b_6 = -0.0772509501792649549463874931821$
	$a_7 = -0.194208871063049124066394765282$	$b_7 = -0.00264758266409925952822161203471$
	$a_8 = -0.323496751337931087309823477561$	$b_8 = -0.0329844384945603065320797537355$
	$a_9 = 0.322817287614899749216601693799$	$b_9 = 0.0476781560950366927530646289755$
	$a_{10} = 1 - 2 \sum_{i=1}^9 a_i$	$b_{10} = \frac{1}{2} - \sum_{i=1}^9 b_i$

Table 5: Coefficients of 8th-order RKN splitting methods of type \mathcal{B}_s , with $s = 17, 18$ and 19 stages.

- \mathcal{O}_{17} : the RKN splitting method of type \mathcal{A}_s presented in [23], with $s = 17$ stages.
- \mathcal{SS}_{17} : the symmetric composition of $m = 17$ symmetric 2nd-order methods of the form (1.8) obtained in [15] (the coefficients are also collected in [11, p. 157]).
- \mathcal{SS}_{19} and \mathcal{SS}_{21} : schemes (1.8) with $m = 19$ and $m = 21$, respectively, presented in [25].

These \mathcal{SS}_m methods have been shown to be the most efficient 8th-order schemes within the family of compo-

sition methods (1.8). We collect in Table 6 the corresponding values of the quantities E_f and Δ for methods \mathcal{SS}_m when they are used with $\mathcal{S}_h^{[2]}$ as in (1.6) (ABA) or (1.7) (BAB). The values of E_f are always greater when the basic scheme is (1.7).

The implementation of all the integrators has been done in Python 3.7 [27] running on Debian GNU/Linux 10 [16] and the array operations have been coded using the *NumPy* library [13].

	E_f		Δ
	ABA	BAB	
\mathcal{O}_{17}	4.78	–	16.63
\mathcal{SS}_{17}	3.12	3.30	8.33
\mathcal{SS}_{19}	2.66	2.68	6.84
\mathcal{SS}_{21}	2.59	2.88	6.43

Table 6: Effective error E_f and 1-norm of the vector of coefficients for 8th-order symmetric compositions of symmetric methods \mathcal{SS}_m and the RKN splitting method of [23].

Example 1: Kepler problem. We take the 2-body gravitational problem with Hamiltonian

$$H(q, p) = \frac{1}{2}p^T p - \mu \frac{1}{r}, \tag{4.1}$$

where $q = (q_1, q_2), p = (p_1, p_2), \mu = GM, G$ is the gravitational constant and M is the sum of the masses of the two bodies. We take $\mu = 1$ and initial conditions

$$q_1(0) = 1 - e, \quad q_2(0) = 0, \quad p_1(0) = 0, \quad p_2(0) = \sqrt{\frac{1+e}{1-e}}, \tag{4.2}$$

so that the trajectory corresponds to an ellipse of eccentricity e , with period 2π and energy $E = -\frac{1}{2}$. We first check the order of the new RKN splitting methods and compare their efficiency with respect to \mathcal{O}_{17} . Thus, Figure 1 (left panel) shows the relative error in energy with respect to s/h (which is proportional to the number of force evaluations) for $e = 0.5$ and a final time $t_f = 1000$ for methods of type \mathcal{A}_s , whereas in the right panel we explore the range of eccentricities $0 \leq e \leq 0.8$. All schemes involve the same number of evaluations of the potential in this case. Figure 2 shows analogous results for methods of type \mathcal{B}_s . Notice that the order 8 is clearly visible in the figures and that the new methods are more efficient than \mathcal{O}_{17} . The improvement is particularly prominent for \mathcal{A}_{17} and specially \mathcal{A}_{19} (up to four orders of magnitude for the same value of h/s) and is more moderate for methods \mathcal{B}_s . In fact, all of them show essentially the same performance, which is lower than that of \mathcal{A}_{19} .

We next carry out the same experiment, but in this case we compare the performance of the new schemes \mathcal{A}_{17} and \mathcal{A}_{19} with the previous state-of-the-art symmetric compositions of the Strang splitting $\mathcal{SS}_m, m = 17, 19, 21$. We take the composition (1.6) as the basic $\mathcal{S}_h^{[2]}$ method because it shows the best performance in the numerical experiments. The corresponding results are shown in Figure 3. We notice that \mathcal{A}_{19} is the more efficient method for the whole range of eccentricities explored.

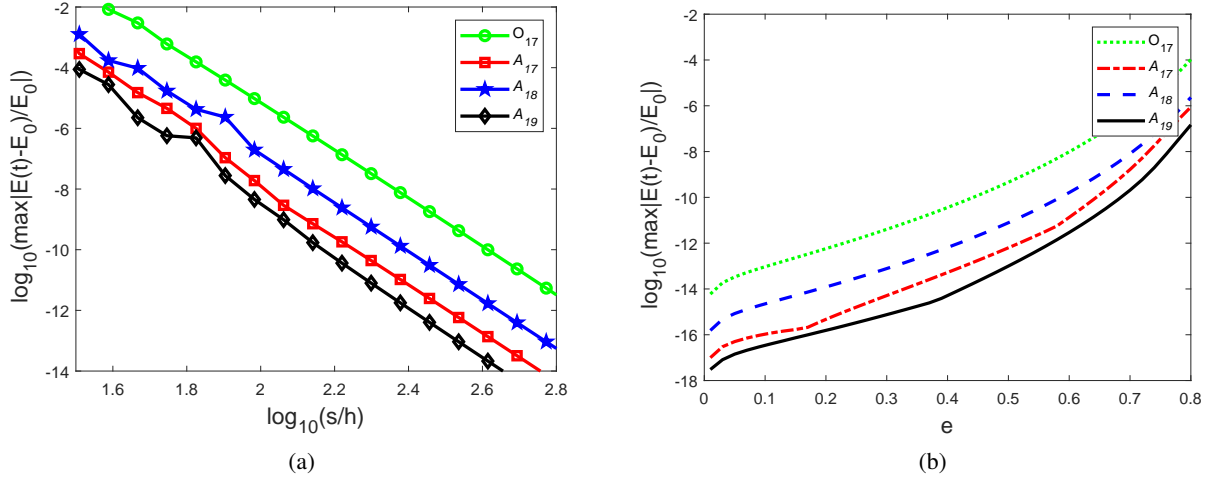


Figure 1: (a) Efficiency diagram for the Kepler problem with $e = 0.5$ for all RKN splitting methods of \mathcal{A}_s type. The final time is $t_f = 1000$. (b) Maximum error in energy for different values of the eccentricity with $t_f = 1000$ and $s/h = 340$.

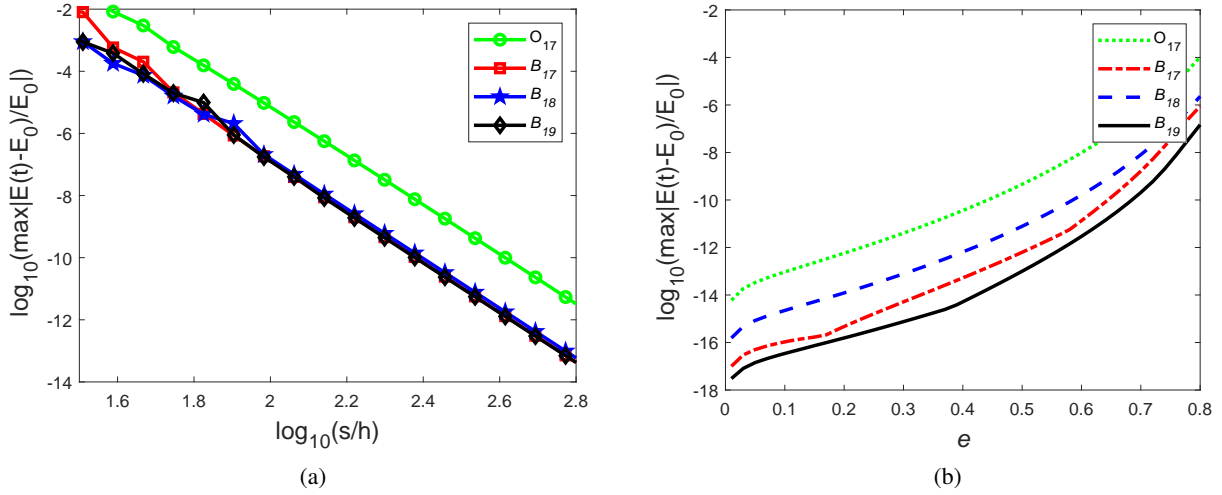


Figure 2: (a) Efficiency diagram for the Kepler problem with $e = 0.5$ for all RKN splitting methods of \mathcal{B}_s type. The final time is $t_f = 1000$. (b) Maximum error in energy for different values of the eccentricity with $t_f = 1000$ and $s/h = 340$.

Example 2: simple pendulum. Our next example is the simple mathematical pendulum. In appropriate units, it corresponds to the 1-degree-of-freedom Hamiltonian system with

$$H(q, p) = \frac{1}{2}p^2 - \cos q. \quad (4.3)$$

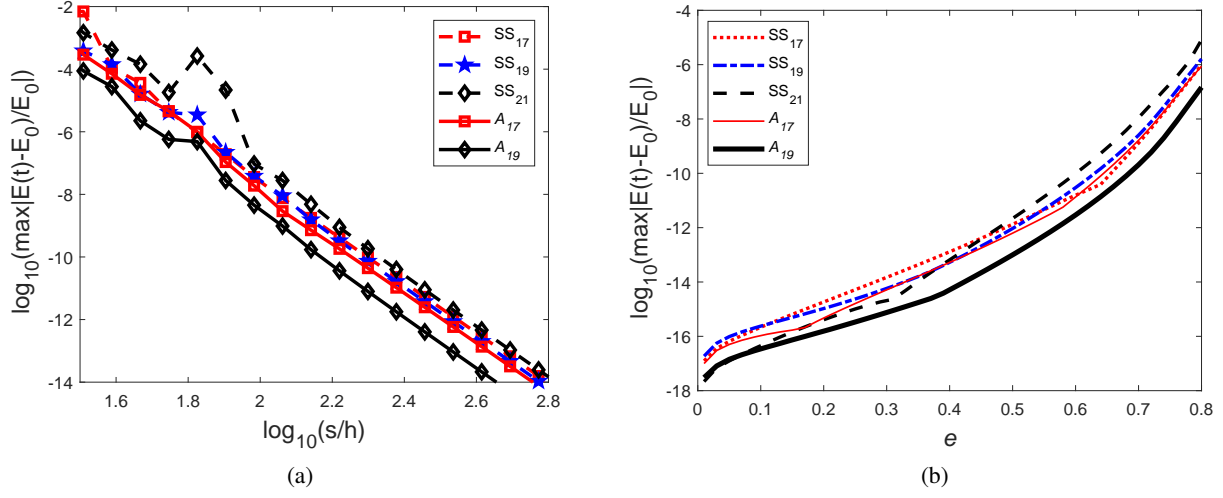


Figure 3: (a) Efficiency diagram for the Kepler problem with $e = 0.5$ for composition SS_m and the new RKN splitting methods \mathcal{A}_{17} and \mathcal{A}_{19} . Final time $t_f = 1000$. (b) Maximum error in energy for different values of the eccentricity with $t_f = 1000$ and $s/h = 340$.

We explore the set of initial conditions $(q, p) = (0, \alpha)$, with $0 \leq \alpha \leq 5$, integrate until the final time $t_f = 1000$ and check the error in energy along the integration. Since the error achieved by \mathcal{O}_{17} is always 3-4 orders of magnitude larger than the new schemes, we no longer include them in the diagrams, so that we only compare with symmetric compositions SS_m . Figure 4 shows the efficiency diagram corresponding to $\alpha = 3$ (panel (a)) and the maximum of the relative error in the energy along the integration interval. In this case, the new schemes \mathcal{A}_{17} and \mathcal{A}_{18} are the most efficient. Scheme \mathcal{A}_{19} shows a similar behavior as SS_{19} , and thus it has not been included in the diagrams. On the other hand, the most efficient scheme of the BAB type in this case is \mathcal{B}_{18} (not shown), providing similar results as \mathcal{A}_{18} .

Example 3: Hénon–Heiles potential. For our next experiment we choose the well known two-degrees of freedom Hénon–Heiles Hamiltonian [14]

$$H = \frac{1}{2}(p_1^2 + p_2^2) + \frac{1}{2}(q_1^2 + q_2^2) + q_1^2 q_2 - \frac{1}{3} q_2^3. \quad (4.4)$$

It has been the subject of extensive numerical experimentation and is considered, in particular, as a model problem to characterize the transition to Hamiltonian chaos. In this case we take the same initial conditions as in [8], the set $(q_1, q_2, p_1, p_2) = (\alpha/2, 0, 0, \alpha/4)$, with $0 \leq \alpha \leq 1$. The corresponding results are depicted in Figure 5. In this case \mathcal{B}_{18} and \mathcal{A}_{18} are the most efficient schemes, whereas \mathcal{A}_{17} is similar as \mathcal{A}_{18} and it is not shown in the figure.

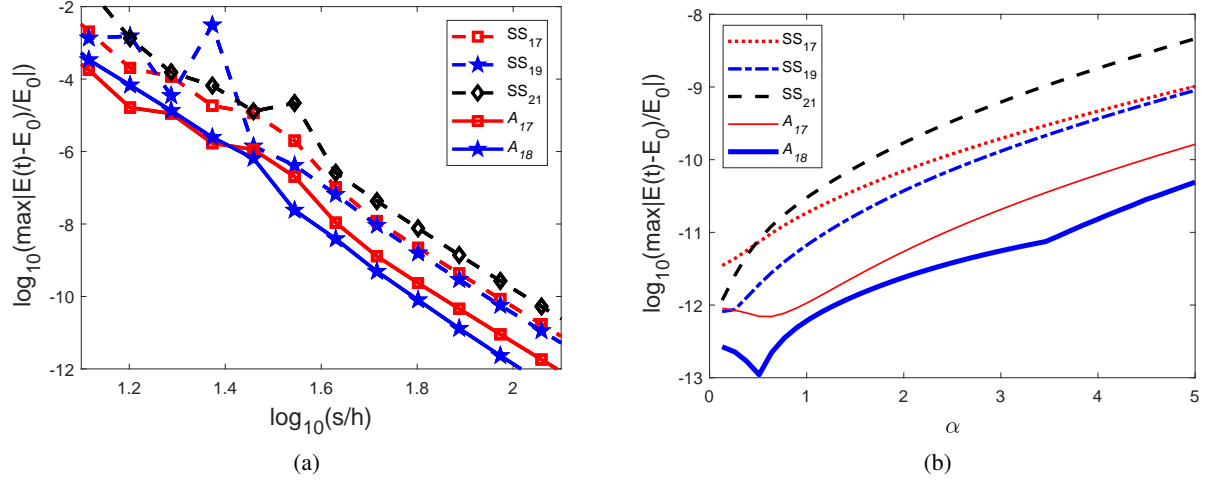


Figure 4: Simple pendulum. (a) Efficiency diagram for $\alpha = 3.0$ and final time $t_f = 1000$. (b) Maximum error in energy for initial conditions $(q_0, p_0) = (0, \alpha)$ for $\mathcal{S}\mathcal{S}$ and the best RKN methods at final time $t_f = 1000$ with $s/h = 85$.

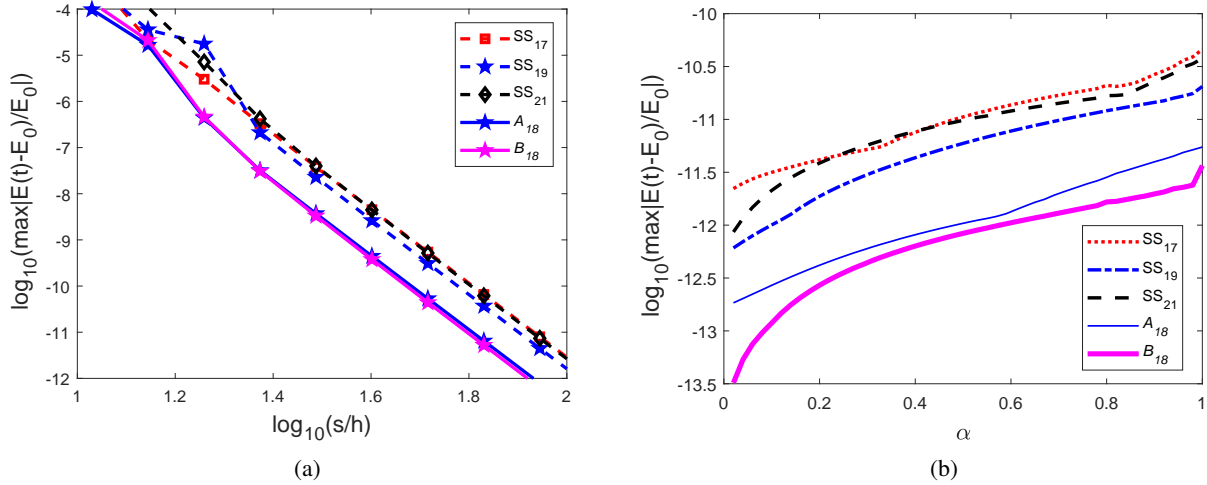


Figure 5: Hénon–Heiles Hamiltonian. (a) Efficiency diagram with initial condition corresponding to $\alpha = 0.2$ and final time $t_f = 1000$. (b) Maximum error in energy for $0 \leq \alpha \leq 1$ at final time $t_f = 1000$ with $s/h = 85$.

Example 4: Schrödinger equation with Pöschl–Teller potential. Finally, we apply our integrators to the one-dimensional Schrödinger equation ($\hbar = 1$)

$$i \frac{\partial}{\partial t} \psi(x, t) = -\frac{1}{2} \frac{\partial^2}{\partial x^2} \psi(x, t) + V(x) \psi(x, t), \quad (4.5)$$

with the well known Pöschl–Teller potential [10],

$$V(x) = -\frac{\lambda(\lambda + 1)}{2} \operatorname{sech}^2(x), \quad (4.6)$$

with $\lambda(\lambda + 1) = 10$. When a Fourier spectral collocation method is used for discretizing in space [26], one ends up with the N -dimensional linear ODE

$$i \frac{d}{dt} u(t) = H u(t) \equiv (T + V) u(t), \quad u(0) = u_0 \in \mathbb{C}^N, \quad (4.7)$$

where T a (full) differentiation matrix related with the kinetic energy, V is a diagonal matrix associated with the potential and the components of the vector u are the approximations to the wave function at the nodes, $u_n \approx \psi(x_n, t)$. The action of T on the wave function vector u is then carried out by the forward and backward discrete Fourier transform (computed with the FFT algorithm) [17]. The initial condition is taken as $\psi_0(x) = \sigma e^{-x^2/2}$, with σ a normalizing constant, the interval is $x \in [-8, 8]$ with $N = 256$ nodes, and the integration is done until the final time $t_f = 1000$. In this case we check the error in the expected value of the energy,

$$\text{energy error: } |u_{\text{ap}}^*(t) \cdot (H u_{\text{ap}}(t)) - u_0^* \cdot (H u_0)|, \quad (4.8)$$

where $u_{\text{ap}}(t)$ stands for the numerical approximation obtained by each method. The results are shown in Figure 6. Observe that the new RKN splitting method \mathcal{A}_{19} is also the most efficient in this setting.

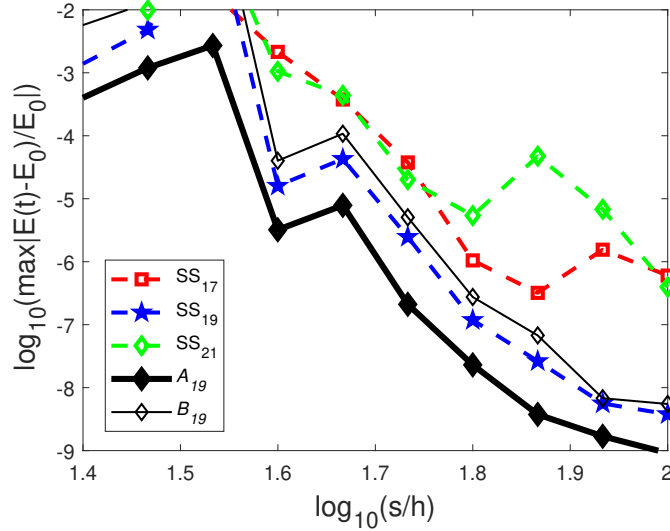


Figure 6: Efficiency diagram of different methods. Schrödinger equation with Pöschl–Teller potential.

5 Numerical tests II: RKN splitting and extrapolation methods

Given the observed improvement of the new 8th-order RKN splitting methods with respect to the symmetric compositions of a basic 2nd-order symmetric scheme, it seems appropriate to carry out further comparisons

with other lower-order RKN splitting methods when medium to high accuracy is desired. Specifically we consider the following optimized 4th- and 6th-order methods of type \mathcal{B}_s presented in [8]:

- RKN4₆: order 4 with 6 stages (the scheme SRKN₆^b in [8]).
- RKN6₁₁: order 6 with 11 stages (the scheme SRKN₁₁^b in [8]).

On the other hand, extrapolation methods constitute one of the most efficient classes of schemes for the numerical integration of the second order differential equation (1.1) when high accuracy is required [12]. Notice, however, that in contrast with RKN splitting methods, they do not preserve by construction geometric properties of the exact solution. To carry out our comparisons, we take (1.6) as the symmetric second order basic method (which corresponds to *Störmer's rule* [12, eq. (14.32)]) and apply the harmonic sequence to construct by extrapolation schemes of orders 4, 6 and 8 with only 3, 6 and 10 stages, respectively. For completeness, the resulting methods can be written explicitly as

$$\Psi_{(r=2k)} = \sum_{\ell=1}^k \alpha_{\ell}^{(k)} \prod_{i=1}^{\ell} \mathcal{S}_{h/\ell}^{[2]}, \quad k = 2, 3, 4,$$

with $\alpha^{(k)} = (\alpha_1^{(k)}, \dots, \alpha_k^{(k)})$ and

$$\alpha^{(2)} = \left(-\frac{1}{3}, \frac{4}{3}\right), \quad \alpha^{(3)} = \left(\frac{1}{24}, -\frac{16}{15}, \frac{81}{40}\right), \quad \alpha^{(4)} = \left(-\frac{1}{360}, \frac{16}{45}, -\frac{729}{280}, \frac{1024}{315}\right). \quad (5.1)$$

Example 5: Kepler problem revisited. For the Hamiltonian (4.1) with initial conditions (4.2) we compare the most efficient 8th-order RKN splitting method \mathcal{A}_{19} with the 4th- and 6th-order schemes RKN4₆ and RKN6₁₁, and the previous extrapolation methods of orders 4, 6 and 8 for the final time $t_f = 1000$. The results achieved for the maximum error in energy and positions are displayed in Figure 7. To reduce round-off errors when computing the linear combinations in extrapolation methods, instead of evaluating directly the numerical solution as $y_{n+1} = \Psi_{(r=2k)} y_n$, we express $y_{n+1}^{(\ell)} \equiv \prod_{i=1}^{\ell} \mathcal{S}_{h/\ell}^{[2]} y_n$ as $y_{n+1}^{(\ell)} = y_n + \Delta y_{n+1}^{(\ell)}$. In this way we compute only $\Delta y_{n+1}^{(\ell)}$, then extrapolation is used only for these increments, namely,

$$\Delta y_{n+1} = \sum_{\ell=1}^k \alpha_{\ell}^{(k)} \Delta y_{n+1}^{(\ell)}$$

and finally we form $y_{n+1} = y_n + \Delta y_{n+1}$. In doing so, round-off errors are reduced by two or more digits.

Figure 7 shows that the new RKN splitting methods are competitive with extrapolation methods and, in particular, \mathcal{A}_{19} is the most efficient when medium to high accuracy is desired.

Example 6: simple pendulum revisited. Let us consider again the simple pendulum, this time with initial conditions $(q, p) = (0, 0.3)$. We measure the error in energy along the integration for the schemes RKN4₆, RKN6₁₁, \mathcal{A}_{18} and the extrapolation methods until the final time $t_f = 1000$. Figure 8 shows the efficiency diagram corresponding to the maximum of the relative error in the energy along the integration interval. In this case, the new scheme \mathcal{A}_{18} is the most efficient when high accuracy is desired. There are initial conditions, however, for which RKN6₁₁ provides better results up to round-off.

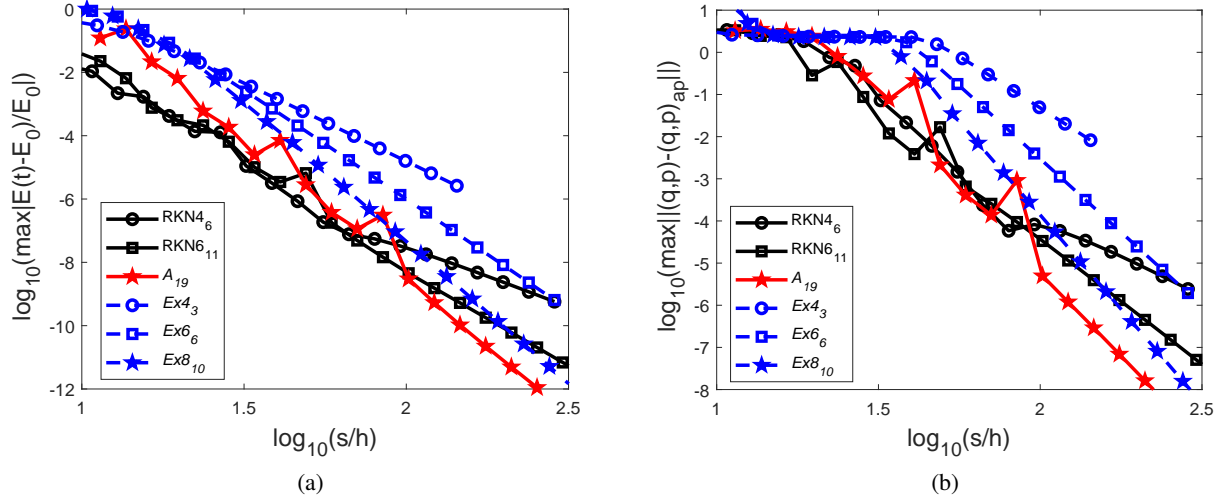


Figure 7: (a) Maximum error in the energy for the Kepler problem with $e = 0.5$ obtained by RKN splitting methods $RKN4_6$, $RKN6_{11}$, \mathcal{A}_{19} (solid lines), and extrapolation (dashed lines) of orders 4 (circles), 6 (squares) and 8 (stars). (b) Same for the maximum error in position.

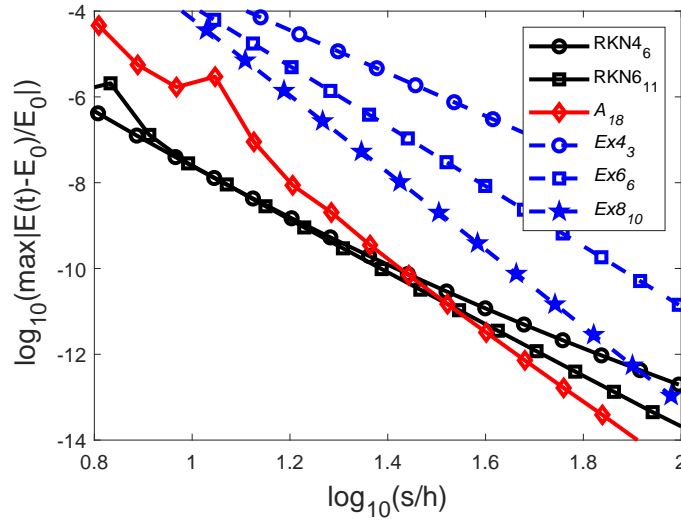


Figure 8: Simple pendulum. Maximum error in the energy for the simple pendulum with initial conditions $(q, p) = (0, 0.3)$ and final time $t_f = 1000$ obtained by RKN splitting methods $RKN4_6$, $RKN6_{11}$, \mathcal{A}_{19} (solid lines), and extrapolation (dashed lines) of orders 4 (circles), 6 (squares) and 8 (stars).

Very similar results are obtained for the Hénon-Heiles potential, and for this reason they are not shown here. From the previous experiments, we can conclude that the new scheme \mathcal{A}_{19} outperforms the symplectic

methods of order 4 and 6 from medium to high accuracy when the potential has a singularity, whereas \mathcal{A}_{17} , \mathcal{A}_{18} and \mathcal{B}_{18} deliver the best results only at high accuracy for smooth potentials. To provide further evidence to this class, we next consider a slightly more involved example.

Example 7: the restricted three body problem. In this case we have two bodies of masses $1 - \mu$ and μ in circular rotation in a plane and a third body of negligible mass moving around in the same plane. The equations of motion in a fixed coordinate system read [12, p. 129]

$$\begin{aligned}\ddot{y}_1 &= y_1 + 2\dot{y}_2 - \mu' \frac{y_1 + \mu}{D_1} - \mu \frac{y_1 - \mu'}{D_2} \\ \ddot{y}_2 &= y_2 - 2\dot{y}_1 - \mu' \frac{y_2}{D_1} - \mu \frac{y_2}{D_2},\end{aligned}\tag{5.2}$$

where $D_1 = ((y_1 + \mu)^2 + y_2^2)^{3/2}$, $D_2 = ((y_1 - \mu')^2 + y_2^2)^{3/2}$, and $\mu' = 1 - \mu$. This system can be split as in (1.9)-(1.10). Alternatively, in a rotating system the equations of motion become

$$\begin{aligned}\ddot{y}_1 &= \mu' \frac{a_1(t) - y_1}{D_1} + \mu \frac{b_1(t) - y_1}{D_2} \\ \ddot{y}_2 &= \mu' \frac{a_2(t) - y_2}{D_1} + \mu \frac{b_2(t) - y_2}{D_2},\end{aligned}\tag{5.3}$$

where now

$$D_1 = ((y_1 - a_1(t))^2 + (y_2 - a_2(t))^2)^{3/2}, \quad D_2 = ((y_1 - b_1(t))^2 + (y_2 - b_2(t))^2)^{3/2},$$

and the motion of the massive bodies is described by

$$a_1(t) = -\mu \cos(t), \quad a_2(t) = -\mu \sin(t); \quad b_1(t) = \mu' \cos(t), \quad b_2(t) = \mu' \sin(t).$$

We take, as in [12], $\mu = 0.012277471$ and the following initial conditions in the rotating system:

$$y_1(0) = 0.994, \quad \dot{y}_1(0) = 0, \quad y_2(0) = 0, \quad \dot{y}_2(0) = -1.00758510637908252240.$$

The resulting closed trajectory corresponds to the so-called Arenstorf orbit in the fixed coordinate system, with period $T = 17.06521656015796255889$.

In this case we integrate for one period with the RKN splitting methods of order 4 and 6, and the new 8th-order scheme \mathcal{A}_{19} . We measure the error with respect to the initial conditions (taking into account that we are integrating in the rotating system) and display the corresponding errors in Figure 9. Again, \mathcal{A}_{19} is the most efficient scheme even for medium accuracies.

6 Conclusions

We have presented new RKN splitting methods of order 8 that show a better efficiency than the best existing symmetric compositions of 2nd-order symmetric schemes on a variety of examples. We have thus answered in the affirmative the question formulated by [21] in 1996 and filled the existing gap in the classification of the most efficient splitting and composition methods [5, 19]. The technical difficulties involved in the process

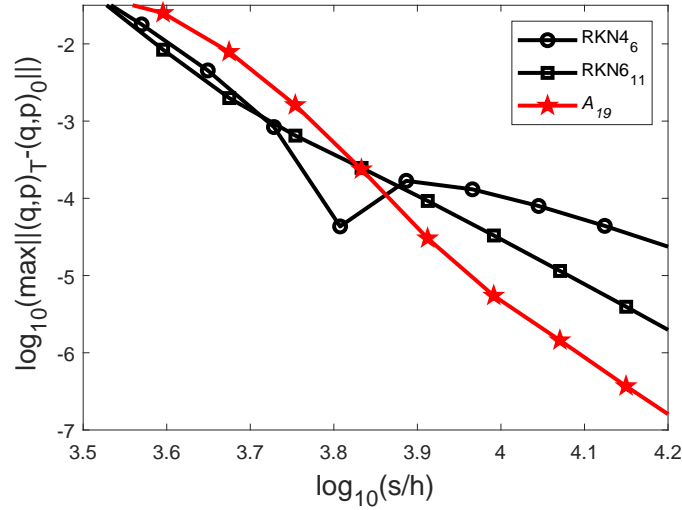


Figure 9: Error with respect to the initial conditions after one period, T , of the Arenstorf orbit versus the number of force evaluations for the 4th-, 6th- and 8th-order RKN splitting methods, $RK4N_6$ (circles), $RKN6_{11}$ (squares) and \mathcal{A}_{19} (stars).

have been overcome by applying standard techniques for solving nonlinear polynomial equations and free software on a personal computer. Whereas previous 8th-order RKN splitting methods require the evaluation of ‘modified potentials’ or force-gradients [24], the schemes collected here only involve the evaluation of the force $g(y)$, just as compositions (1.8) and thus they should be considered as the natural option when one is interested in integrating the system (1.1) with high precision and the evaluation of modified potentials is computationally expensive or not feasible.

Both types of compositions (2.4) and (2.5) have been analyzed and different schemes with up to two free parameters have been constructed and tested on different numerical examples. These show that \mathcal{A}_{18} and \mathcal{B}_{18} provide better efficiencies when the force is derived from a smooth, singularity-free potential, whereas for problems involving singularities \mathcal{A}_{19} exhibits the best results. Moreover, they are more efficient than lower order RKN splitting methods for medium to high accuracies, and provide better results than extrapolation methods of order 8 even for relatively short time integrations.

Acknowledgements

This work has been supported by Ministerio de Ciencia e Innovación (Spain) through project PID2019-104927GB-C21, MCIN/AEI/10.13039/501100011033. A.E.-T. has been additionally funded by the predoctoral contract BES-2017-079697 (Spain). A.E.-T. would like to thank Ander Murua and Joseba Makazaga for their help in implementing their continuation algorithms and the UPV-EHU for its hospitality.

References

- [1] <https://github.com/jmakazaga/arc-continuation>

- [2] E. ALBERDI, M. ANTOÑANA, J. MAKAZAGA, AND A. MURUA, *An algorithm based on continuation techniques for minimization problems with highly non-linear equality constraints*, Tech. Rep. arXiv:1909.07263, 2019.
- [3] V. ARNOLD, *Mathematical Methods of Classical Mechanics*, Springer-Verlag, Second ed., 1989.
- [4] S. BLANES AND F. CASAS, *A Concise Introduction to Geometric Numerical Integration*, CRC Press, 2016.
- [5] S. BLANES, F. CASAS, AND A. MURUA, *Splitting and composition methods in the numerical integration of differential equations*, Bol. Soc. Esp. Mat. Apl., 45 (2008), pp. 89–145.
- [6] S. BLANES, F. CASAS, AND J. ROS, *High-order Runge–Kutta–Nyström geometric methods with processing*, Appl. Numer. Math., 39 (2001), pp. 245–259.
- [7] S. BLANES, F. CASAS, AND J. ROS, *New families of symplectic Runge–Kutta–Nyström integration methods*, in Numerical Analysis and its Applications, LNCS 1988, Springer, 2001, pp. 102–109.
- [8] S. BLANES AND P. MOAN, *Practical symplectic partitioned Runge–Kutta and Runge–Kutta–Nyström methods*, J. Comput. Appl. Math., 142 (2002), pp. 313–330.
- [9] M. CALVO AND J. SANZ-SERNA, *High-order symplectic Runge–Kutta–Nyström methods*, SIAM J. Sci. Comput., 14 (1993), pp. 1237–1252.
- [10] S. FLÜGGE, *Practical Quantum Mechanics*, Springer, 1971.
- [11] E. HAIRER, C. LUBICH, AND G. WANNER, *Geometric Numerical Integration. Structure-Preserving Algorithms for Ordinary Differential Equations*, Springer-Verlag, Second ed., 2006.
- [12] E. HAIRER, S. NØRSETT, AND G. WANNER, *Solving Ordinary Differential Equations I, Nonstiff Problems*, Springer-Verlag, Second revised ed., 1993.
- [13] C. R. HARRIS, K. J. MILLMAN, S. J. VAN DER WALT, R. GOMMERS, P. VIRTANEN, D. COUNAPEAU, E. WIESER, J. TAYLOR, S. BERG, N. J. SMITH, R. KERN, M. PICUS, S. HOYER, M. H. VAN KERKWIJK, M. BRETT, A. HALDANE, J. FERNÁNDEZ DEL RÍO, M. WIEBE, P. PETERSON, P. GÉRARD-MARCHANT, K. SHEPPARD, T. REDDY, W. WECKESSER, H. ABBASI, C. GOHLKE, AND T. E. OLIPHANT, *Array programming with NumPy*, Nature, 585 (2020), p. 357–362.
- [14] M. HÉNON AND C. HEILES, *The applicability of the third integral of motion: some numerical experiments*, Astron. J., 69 (1964), pp. 73–79.
- [15] W. KAHAN AND R. LI, *Composition constants for raising the order of unconventional schemes for ordinary differential equations*, Math. Comput., 66 (1997), pp. 1089–1099.
- [16] M. F. KRAFFT, *The Debian System: Concepts and Techniques*, No Starch Press, 2005.
- [17] C. LUBICH, *From Quantum to Classical Molecular Dynamics: Reduced Models and Numerical Analysis*, European Mathematical Society, 2008.

- [18] R. MCLACHLAN AND A. MURUA, *The Lie algebra of classical mechanics*, J. Comput. Dyn., 6 (2019), pp. 198–213.
- [19] R. MCLACHLAN AND R. QUISPTEL, *Splitting methods*, Acta Numerica, 11 (2002), pp. 341–434.
- [20] R. MCLACHLAN AND B. RYLAND, *The algebraic entropy of classical mechanics*, J. Math. Phys., 44 (2003), pp. 3071–3087.
- [21] R. MCLACHLAN AND C. SCOVEL, *A survey of open problems in symplectic integration*, in Integration Algorithms and Classical Mechanics, J. Marsden, G. Patrick, and W. Shadwick, eds., Fields Institute Communications, American Mathematical Society, 1996, pp. 151–180.
- [22] J. J. MORÉ, B. S. GARBOW, AND K. E. HILLSTROM, *User guide for MINPACK-1*, tech. rep., CM-P00068642, 1980.
- [23] D. OKUNBOR AND E. LU, *Eighth-order explicit symplectic Runge–Kutta–Nyström integrators*, Tech. Rep. CSC 94-21, University of Missouri-Rolla, 1994.
- [24] I. OMELIAN, I. MRYGLOD, AND R. FOLK, *On the construction of high order force gradient algorithms for integration of motion in classical and quantum systems*, Phys. Rev. E, 66 (2002), p. 026701.
- [25] M. SOFRONIOU AND G. SPALETTA, *Derivation of symmetric composition constants for symmetric integrators*, Optim. Method. Softw., 20 (2005), pp. 597–613.
- [26] L. TREFETHEN, *Spectral Methods in MATLAB*, SIAM, 2000.
- [27] G. VAN ROSSUM AND F. L. DRAKE, *Python 3 Reference Manual*, CreateSpace, Scotts Valley, CA, 2009.
- [28] V. VARADARAJAN, *Lie Groups, Lie Algebras, and Their Representations*, Springer-Verlag, 1984.
- [29] P. VIRTANEN, R. GOMMERS, T. E. OLIPHANT, M. HABERLAND, T. REDDY, D. COURNAPEAU, E. BUROVSKI, P. PETERSON, W. WECKESSER, J. BRIGHT, S. J. VAN DER WALT, M. BRETT, J. WILSON, K. J. MILLMAN, N. MAYOROV, A. R. J. NELSON, E. JONES, R. KERN, E. LARSON, C. J. CAREY, Í. POLAT, Y. FENG, E. W. MOORE, J. VANDERPLAS, D. LAXALDE, J. PERKTOLD, R. CIMRMAN, I. HENRIKSEN, E. A. QUINTERO, C. R. HARRIS, A. M. ARCHIBALD, A. H. RIBEIRO, F. PEDREGOSA, P. VAN MULBREGT, AND SCIPY 1.0 CONTRIBUTORS, *SciPy 1.0: Fundamental algorithms for scientific computing in Python*, Nature Methods, 17 (2020), pp. 261–272.